2015

Acoustic emission monitoring of multi-phase fluid flow in laser-engineered net shaping process (LENS)

Justin Whiting

ABSTRACT

ACOUSTIC EMISSION MONITORING OF MULTI-PHASE FLUID FLOW IN LASER-ENGINEERED NET SHAPING PROCESS

Justin Whiting, M.S.
Department of Mechanical Engineering
Northern Illinois University, 2015
Federico Sciammarella, Director

The laser-engineered net shaping (LENS) process uses an argon stream to direct metallic particulates at a molten pool created by a high-power Yb-fiber laser. The LENS process uses numerical control (NC) to manipulate the laser beam heat source in 3-dimensional space so parts can be built additively, layer-by-layer. The metal powder that is carried by the stream of argon gas creates a two-phase fluid, which can make measurement of mass flow rate difficult using conventional sensors. Maintaining a specified mass flow rate is essential in the quality control of this additive manufacturing process. An alternative device, an acoustic emission (AE) sensor, is proposed to monitor the rate of the metal powder flowing through the machine's nozzles. Pressure waves are created by the collisions of the powder with one another as well as the walls of the channel. This pressure is transduced by the piezo-electric element in the base of the AE sensor into electro-motive force. A mount was designed and created to facilitate non-intrusive

flow monitoring using AE. The actual mass is monitored using a scale and a powder capture apparatus. The real mass over time and the RMS of the AE signal are compared and found to correlate closely. The system will be implemented in Optomec's LENS 850-M machine in order to provide feedback to the machine's operator regarding the condition of the powder delivery system. The relationship between the AE RMS and the actual flow rate will be characterized and used to estimate the actual flow using only AE. Further research is conducted on the frequency spectrum of the AE waveform, and a control system will be proposed.

NORTHERN ILLINOIS UNIVERSITY
DE KALB, ILLINOIS

MAY 2015

ACOUSTIC EMISSION MONITORING OF MULTI-PHASE FLUID FLOW IN LASER-ENGINEERED NET SHAPING PROCESS (LENS)

BY

JUSTIN WHITING

A THESIS SUBMITTED TO THE GRADUATE SCHOOL

IN PARTIAL FULFILLMENT OF THE REQUIREMENTS

FOR THE DEGREE

MASTER OF SCIENCE

DEPARTMENT OF MECHANICAL ENGINEERING

Thesis Director:

Federico Sciammarella

ACKNOWLEDGEMENTS

The work I have completed for this report would not be possible without the guidance of the faculty at Northern Illinois University, particularly the College of Engineering and Engineering Technology. Thank you to Dr. Sciammarella, Dr. Gonser, and Dr. Santner for providing this opportunity and generously offering their time and expertise. Thank you to the National Institute of Standards and Technology (NIST) for providing the funding for this research project and many others that allow the U.S. and the world to advance emerging technologies. Finally, thanks go to all of the research assistants that are part of ARMM© (Advanced Research of Materials and Manufacturing) Lab.

TABLE OF CONTENTS

Page

Page

LIST OF FIGURES

Page

Page

LIST OF APPENDICES

Page

CHAPTER 1. INTRODUCTION

1.1 Laser-Engineered Net Shaping

Additive manufacturing (AM), also known as 3D printing, has been experiencing enormous growth over the past few years. The 3-D printing products and services sector had around 29% growth in 2012 [1]. This rapid growth signifies a shift in the manner in which the products consumed are created. While the majority of additive manufacturing processes use a polymer build material, a few are utilizing metallic alloys. The laser-engineered net shaping (LENS) process is one of these processes. The LENS process, developed at Sandia National Laboratory, provides the operator with the means to produce metal components layer by layer taking a CAD drawing to a final product without using traditional subtractive manufacturing methods [2]. This effectively cuts waste, reduces creation time, and can be used to add material to existing parts.

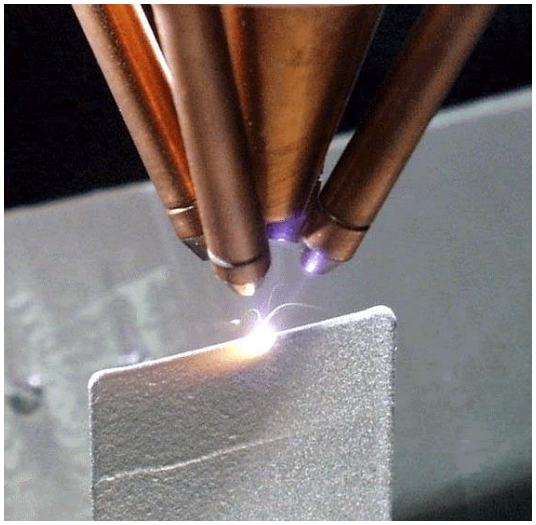

Figure 1: Powder Delivery in LENS [2]

The process uses argon as both a shielding and carrier of the build powder. The powder is projected into a molten pool created in the substrate by a high powered laser. As the depositing head transverses, the molten pool rapidly solidifies creating a dense deposited bead. As the additive manufacturing industry enters the future, various methods of quality control will be needed. Condition monitoring tools are essential to ensure high quality part production.

1.2 Acoustic Emission

Acoustic emission refers to a "transient elastic (stress) wave generated by the rapid release of energy from a localized source" [3]. The emission is a pressure wave given off due to stress usually as a result of an applied load or change in load. The term can be misleading as the usual frequency range considered as AE is from 100 kHz to 2 MHz, far above audible levels of the 20 Hz to 20 kHz range of the human ear. Acquiring data in higher frequency spectrums avoids confusion with noise as most machinery noise is at relatively low frequencies. Acoustic emission is widely used as a tool for various industrial applications which include, but are not limited to, structural integrity of bridges, weld condition monitoring, aerospace structure monitoring, pressure vessel corrosion detection, and various other condition monitoring techniques [3-6].

1.3 Micro-end-mill Tool Wear and AE

DARPA funded research was conducted to determine the feasibility of using AE as a tool-condition monitoring device during the micro end milling of steel [7]. High-speed video, micrography, and acoustic emission were used to characterize the progression of wear throughout the duration of a micro end mill's life. The acoustic emission waveform was found

to be correlated with the wear of the end mill. Although the results were promising, the lack of repeatable tool durations proved the prediction of catastrophic failure implausible. These difficulties were attributed to the heterogeneity in the grain structure of the steel. AE has been shown to be useful in macro machining, but the minute nature of the cutting tool creates convoluted relationships between the dynamics of the tool's flutes and the work piece. Whereas the material removal in macro machining can be modeled as relatively steady, the manner in which each flute enters the material can generate wildly varying forces depending on the location of entry. These fluctuations create impulse-like loads on the tool, causing failure. Though utilizing AE as a method to predict failure proved quite difficult, the insight gained by the research allowed for substantially longer tool durations by optimizing the rotational speed, travel speed, and the dynamics of each flute pass.

1.4 AE for Bulk Condition Monitoring during LENS Process

The direction of the work detailed in this report began with the investigation of using AE as a bulk condition monitoring tool. The exploratory research aimed to use an AE sensor mounted to the substrate to provide data on the condition of the build. The main focus was on the detection of pores, voids, and any other undesirable defects. The research aimed to detect micro-voids with sizes ranging from 1-70 μm. While many other techniques of characterizing the build quality exist (e.g. CT scan, x-ray, SEM, EBSD), nearly all of them have the limitation of needing the part to be completed and often physically removed from the substrate. In fact, many of them require the destruction of the part (i.e. destructive testing). For this reason, the use of a non-destructive testing method such as AE was utilized. Figure 2 is a representation of the

setup used in the research. The AE sensor picks up the emitted waves from the LENS process. The noise created by the powder projected proved to be an insurmountable obstacle. Not only does the powder directed into the melt pool create AE, but AE is also produced by unsolidified powder projection as well as residual powder that is blown by the stream of argon shielding gas. Various signal processing techniques, including frequency bandwidth filtering, location filtering, and signal-noise moving thresholds, were implemented in the hopes of removing noise created by the powder. Even with the filtering, the presence of voids could not be detected. It is likely the voids were not creating any AE. In other words, the attempt to detect them was effectively a search for the lack of AE. The AE was found to closely correlate with the amount of powder projected. For these reasons, the conclusion was reached that AE was best used as a tool for tracking the amount of powder carried through the system's tubing.

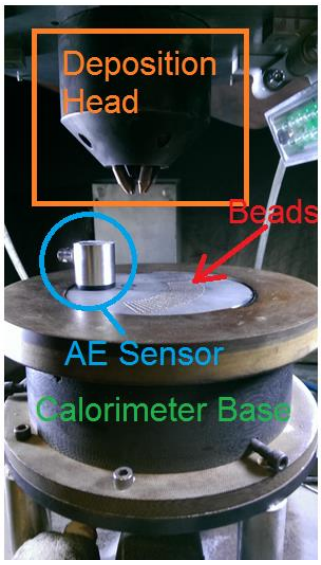

Figure 2: AE as LENS Condition Tool

1.5 Multiphase Mass Flow Rate

The need for the ability to measure the flow rate of a multi-phase fluid is prevalent in the oil, fracking, pulverized fuel delivery, steel production, food processing, chemical, cement production and many other industries [8]. Most of the current methods of measuring the flow rate are restricted to invasive methods, while many of the non-invasive lack accuracy [9]. These conventional methods use empirical results relying on trial and error to attain appropriate operating conditions. This type of measurement is not applicable in the LENS powder delivery system due to its sensitive nature. Any impedance in the flow, like that created by a turbine flow meter, will alter the amount of powder conveyed, therefore changing the build quality. Furthermore, the system is in need of a robust flow meter capable of accurately monitoring a dilute phase flow (i.e. build particles suspended in argon carrying gas) as well as a flow with a high percentage of solid to gaseous [10]. Numerous books and research ventures are invested in describing the manner in which granular material flows [11] and how each particle interacts with other particles and their environment [12]. While characterizing the flow is important, there is a need for an in-situ feedback tool describing the flow of the powder.

1.6 Powder Feeder

The LENS process uses build particles of various sizes and types. The process must have a continuous, steady delivery of the powdered build material in order to ensure a high quality build. This is the responsibility of the machine's powder feeder. Through a combination of mechanical and pneumatic feeding, the powder is conveyed. The hopper holds the powder at a constant pressure. An auger below the hopper's outlet directs the powder into a wheel. The

wheel has small holes that carry the powder in a circular matter. Once the powder reaches the NE section, an argon stream carries the powder into the tubes. This creates a two-phase fluid that has a consistent velocity. The amount of solid build particulates changes with the rotational speed of the feeder's motor. While in theory this should provide a relatively consistent flow, the flowability, moisture content, geometries, and surface friction coefficients all play a role in the manner in which the material is conveyed [11-12]. A reliable measurement of the actual mass flow rate of the build powder is the first step to controlling this flow.

1.7 Summary

The LENS, like all other manufacturing processes, must have methods of quality control in place to ensure a preferable outcome. Inconsistent powder delivery can cause inaccurate build geometries which can compound when the laser's focal point is no longer at a solid surface. The amount of build powder conveyed should be controlled actively, but the first step in doing this is implementing an accurate sensor that provides feedback on the actual mass flow rate. This report focuses on work using AE to monitor the two-phase fluid flow that is present in the LENS process. The goal of this research is to create an in-situ flow monitoring device that can provide reliable feedback to the LENS operator. The sensor must be isolated from external noise, able to detect changes of less than .5 grams/min, and produce flow rate data that has greater than a .95 correlation coefficient with the actual mass flow rate. The system created will be implemented in the LENS process to provide feedback on the condition of the powder delivery system.

CHAPTER 2. THEORY

2.1 Acoustic Emission

Acoustic Emission refers to stress waves given off due to the release of energy from an event (e.g.: impact, loading, crack growth or initiation, rubbing, rapid cooling, etc.). An AE sensor is shown in Figure 3. The primary component in the sensor is the piezoelectric element. Piezoelectric refers to the phenomena that takes place in the said material. When an electric potential is applied across the material, the shape of the material changes. This is also true in reverse: an applied pressure (English equivalent of the Latin word piezo) causes a voltage across the material. The latter of these two is the operating principle of AE sensors. The electromotive force (EMF) created by the waves at the surface of the material is transduced by the AE sensor into an EMF which can be recorded by a data acquisition system (DAQ). The remaining components in the actual sensor are necessary to prolong the life of the sensor (e.g. wear plate, case) and improve accuracy (e.g. dampener).

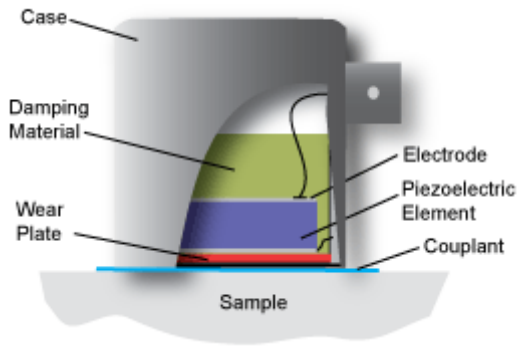

Figure 3: AE Sensor Diagram [5]

The pressure waves are emitted from the source's location and travel throughout the material in various wave modes depending on the geometry and material properties of the medium and, of course, the nature of the event that created the emission. There are several wave modes that describe the manner in which an acoustic wave can travel. Table 1 contains the major wave modes and the manner in which the material moves. In the application described in this report only Rayleigh and longitudinal waves are assumed to be present due both to the manner in which the AE is created as well as the material properties. Due to the complex nature of the attenuation and manners in which the pressure waves travel, most scientists use AE to analyze the data in a statistical approach [5]. The motion of a Rayleigh wave is shown in Figure 4. These waves are considered the major constituent of the AE detected during the powder flow monitoring. This is mainly attributed to the directionality of the sensor used. Figure 5 illustrates the manner in which shear and Love waves travel. The unidirectionality of most AE sensors prohibit the acquisition of motion transverse of the sensor's axis.

Table 1: Wave Modes [5]

Wave Types in Solids	Particle Vibrations
Longitudinal	Parallel to wave direction
Transverse (Shear)	Perpendicular to wave direction
Surface - Rayleigh	Elliptical orbit - symmetrical mode
Plate Wave - Lamb	Component perpendicular to surface (extensional wave)
Plate Wave - Love	Parallel to plane layer, perpendicular to wave direction
Stoneley (Leaky Rayleigh Waves)	Wave guided along interface
Sezawa	Antisymmetric mode

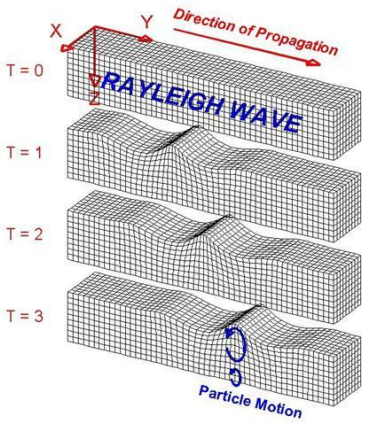

Figure 4: Rayleigh Wave Particle Motion

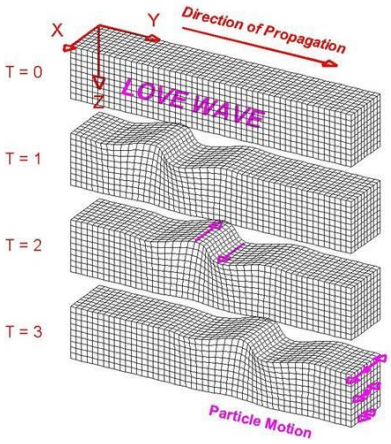

Figure 5: Love Wave

2.2 AE Waveform Analysis

The piezoelectric sensor takes the deformation in the surface of the work piece and sends the electromotive force given off by the piezoelectric element towards an amplifier. As any other waveform, there are various features that can be derived from an acoustic emission signal. All data was collected while monitoring nine AE features that included the five shown in Figure 6 as well as average signal length, average frequency, RMS, signal strength. Note the horizontal line labeled 'Threshold' in Figure 6. This is user-specified and can affect many of the other waveform characteristics. Since an AE 'hit' is only recorded if the signal crosses the threshold, the value chosen will alter not only the amount of counts but even if the data is even stored. A Hsu-Nielson test is used to adjust the threshold to ensure the system is detecting AE of the process being studied [3]. The Hsu Neilson test prescribes breaking of a .5mm diameter pencil lead. The length of the lead should be 3 mm (+/- .5mm) and be pressed against the region of interest until it breaks, emitting pressure waves. The hit-driven nature of AE acquisition also

causes the data to have various sampling intervals which creates the need for a resampling in order to directly compare the AE data to another physical characteristic, such as mass flow rate. After it is amplified, the EMF (measured in volts) is recorded and processed at high frequencies by the Vallen's AMSY-6 AE card alongside the AMSY-6 software. From these voltage and time datum's, various AE features are extracted. The average signal length (ASL) is found by taking the durations of multiple waveforms and finding their average. The measured area under the rectified signal envelope (MARSE) is also known as energy counts, and is simply the integral of the waveform signals produced by the AE event(s).

The RMS of the acoustic emission waveform is calculated using equation (1), where T represents a 6.5ms constant and U(t) is the voltage as a function of time. This mathematical procedure provides a value that does not have an average skewed by negative values. Note the voltage is squared and therefore RMS is always a positive value.

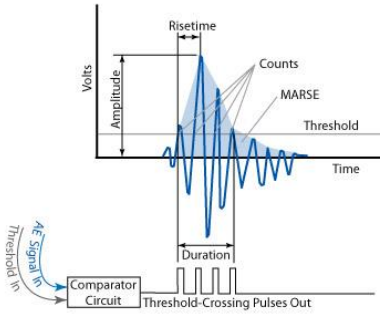

Figure 6: AE Signal Features [5]

$$RMS_{True\ Energy} = \sqrt{\frac{1}{T}\int_0^T U(t)^2 dt} \qquad (1)$$

2.3 Signal Processing

The data acquired from the scale and the RMS of the acoustic emission must be processed in order to extract a useful relationship. The end goal of this work is to provide a tool that uses acoustic emission data to provide an Optomec operator with an accurate measurement of the mass flow rate of the powder traveling through the machine's nozzles. This data can then be compared with the desired flow rate and provide user feedback. The AE data must be appropriately manipulated to accomplish this. A certain function must be extracted that describes the mass flow rate in terms of the RMS of the AE signal. The order of conditioning starts with adjusting the sampling frequency of the AE data. The AE data is compared to the scale's actual mass flow rate, and a lag shift is used to align the signals in the time domain. The final step allows the extraction of a mathematical relationship by means of a least squares regression. Before any of the data can be processed, a smoothing is achieved by calculating a moving average with 77 sample points and assigning this to the mass flow rate array. This was found to provide the best correlation between the datum sets.

2.3.1 Resampling AE Data

The first hurdle is to adjust the sampling frequency of the data sets so that the interval between data points is the same. In order to extract a relationship between the two signals, they must first have equivalent sampling frequencies. In other words, if 100 sample points from the scale data are compared to 100 data points from the AE signal, the time from sample 1 to 100 must be the same on both sample sets. This is accomplished using a native interpolation that Matlab provides. Figure 7 provides an example of how the function works. The algorithm

creates a function that describes the data throughout the time domain plot. For this application, the data is sampled rather quickly and varies rapidly, and therefore a linear interpolation is used. Once the data is interpolated, the user may choose other sampling frequencies with relatively small propagated error. Since the sampling frequency of the scale data was chosen by the user and is consistent, this same frequency is used in the resampling of the AE data. The AE data is hit driven, and therefore does not have consistent sampling frequencies, whereas the scale data is sampled at equal, user-specified intervals.

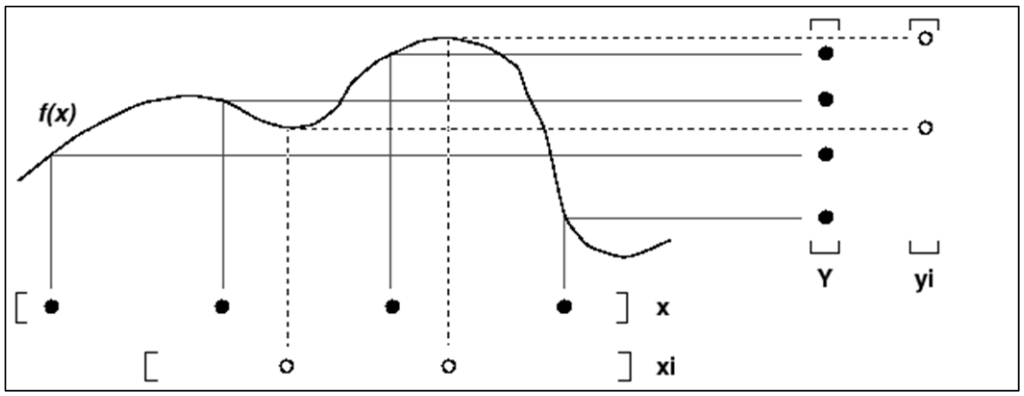

Figure 7: Example of Interpolation from Matlab Help

2.3.2 Lag Shifting

Since the AE data and the scale data must be acquired using different systems, the two data sets must be aligned in terms of their respective times before any further signal manipulation may take place. This is accomplished via a lag shifting using the cross-correlation function in Matlab's library. Cross-correlation is similar to a linear correlation (see equation **(2)**) [13]. This equation provides a value, 'r', that signifies the degree of correlation [13].

Table 2 shows the meaning of the respective 'r' values. The goal of the signal analysis is to provide a function in which the RMS of the AE can be utilized to calculate the mass flow rate. In order to minimize this functions error, the 'r' value must be minimized. This is accomplished using a shift in the function, or a lag shift. The cross-correlation uses the functions $x(t_1)$ and $y(t_2)$, where t_1 and t_2 are two unrelated time arrays, and finds the value of the lag shift, 'τ', that provides the optimal 'r' value.

Equation **(3)** is used to calculate the cross-correlation function, and Figure 8 illustrates how it can be leveraged [14].The cross-correlation compares the integrals of both functions using incrementally changing lags (τ). The cross-correlation value found from equation **(3)** is at a maximum when the lag, τ, minimizes the difference of the two functions' integrals.

$$r = \frac{\sum_i (x_i - \bar{x})(y_i - \bar{y})}{\left(\sqrt{\sum_i (x_i - \bar{x})^2}\right)\left(\sqrt{\sum_i (y_i - \bar{y})^2}\right)} \tag{2}$$

$$R_{xy}(\tau) = \frac{1}{T}\int_0^T x(t)\,y(t+\tau)\,dt \tag{3}$$

Table 2: Correlation Coefficient Meaning

r-Value	Correlation
1	Perfectly Correlated
0	Exactly No Correlation
-1	Perfectly Anti-Correlated

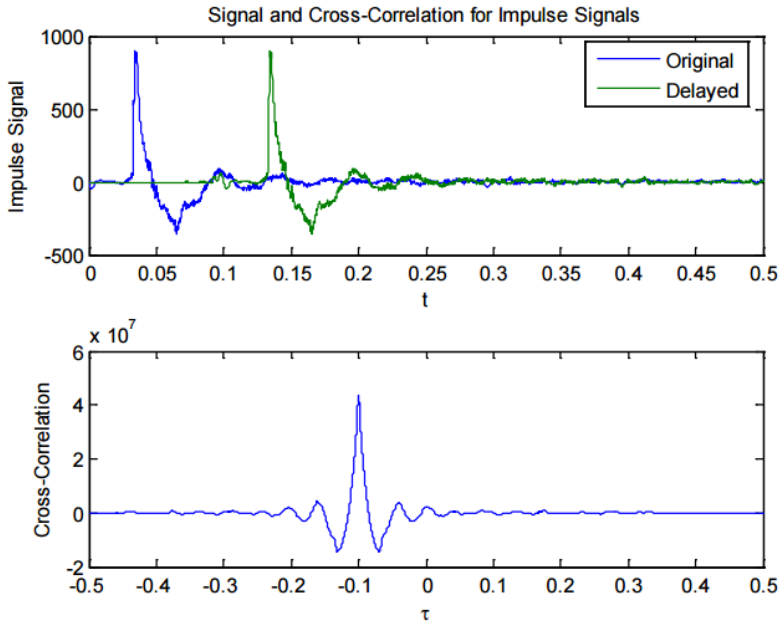

Figure 8: Cross-correlation of Delayed and Original Signal

2.3.3 Least Squares Regression

Least squares regression can be used to assign values to coefficients of an nth ordered polynomial that is used to estimate the value of a certain function. This will provide the means for creating a function that describes the mass flow rate in terms of the RMS of the AE signal. This research will be using the RMS of the AE signal as the input to a function that will estimate the mass flow rate in grams per minute. The mathematics used for a least squares regression are

shown in equation **(4)** [15]. The value of Q is minimized effectively finding values of the coefficients (β) that fit the actual data best. This is accomplished by taking the partial derivative of Q with respect to each of the coefficients and setting them equal to zero (maximum/minimum when slope equals zero). Each partial derivative provides an equation which gives a total of n equations with n unknown variables (β's). The system of equations is solved and the coefficients are found (see equation **(5)**).

$$Q = \sum_{i=1}^{n} [y_i - f(\vec{x}_i; \hat{\vec{\beta}})]^2 \quad (4)$$

$$\frac{\partial Q}{\partial \beta_n} = 0 \quad (5)$$

CHAPTER 3. EXPERIMENTAL SETUP AND PROCEDURE

4.1 Sensor Mount

In order to monitor the flow of the build powder using acoustic emission, there must be a way of allowing the sensor to transduce the surface waves created by the particle collisions. Keeping this goal in mind, several criteria were set: the AE sensor mount must be nonintrusive, provide maximum signal-to-noise, and isolate external noise sources. Below is a bulleted list detailing how each criteria was met, the most vital of which being the minimal distance between sensor and the internal walls of the powder flow's channel. The CAD drawing is shown in Figure 9 and the final mount is shown in Figure 10.

- Mount Design Specifications
    - Nonintrusive
        - Straight bored hole: no curvature or change in diameter causing major head loss and/or potential clogging
        - Smooth continuous inner channel walls: minimal friction minimizes minor head losses, and any voids or cavities would allow powder to rest creating a blockage
        - Minimal length: the shorter the channel the less minor head loss created
    - Maximum signal-to-noise
        - Large sensor base
        - Sensor floor in close proximity to flow channel: less material the waves travel through the less attenuation which can skew results or prevent detection of AE entirely
        - Tightly fitting sensor receiver: any slippage or rubbing can create AE and false readings
    - Noise Isolation
        - Dampener attached to bottom of mount: thick rubber base provides excellent damping of external noises
        - No metal on metal contact with machinery

The design of the mount is straight-forward as shown in Figure 9. On one end, the build material, pneumatically conveyed by argon, enters the body of the mount. The particulates travel through the mount's internal channel, all the while colliding with one another and the walls of the channel, creating AE, and exiting out the outlet. The AE travels through the stainless steel body creating longitudinal and surface (Rayleigh) waves. The sensor, which is coupled to the base, transduces the signal into EMF, which is read into the test equipment at 2 MHz. Both the outlet and inlet have ¼" NPT connections with push-to-connect fittings. The tapered NPT tap provides an airtight seal to ensure no loss of powder or pressure of the carrying gas. Push-to-connect fittings allow the apparatus to quickly and easily be installed or removed. Four counter-bored holes provide the means for the apparatus to be attached to the LENS machine. In order to visualize the manner of the flowing powder, a simple CFD model was created and is shown in Figure 11.

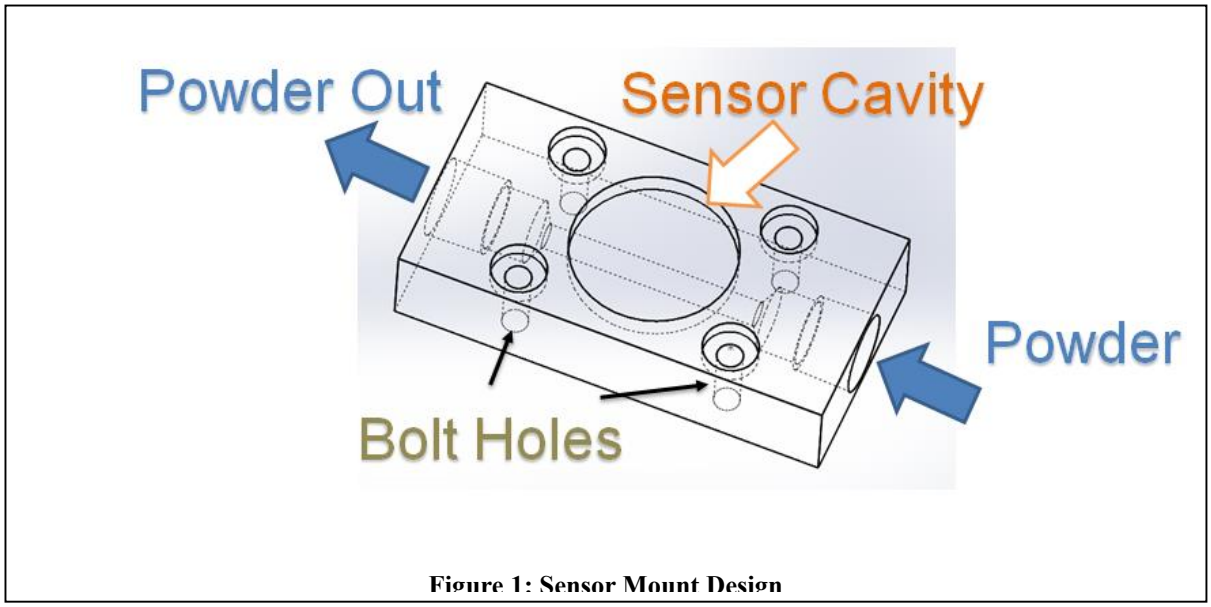

Figure 1: Sensor Mount Design

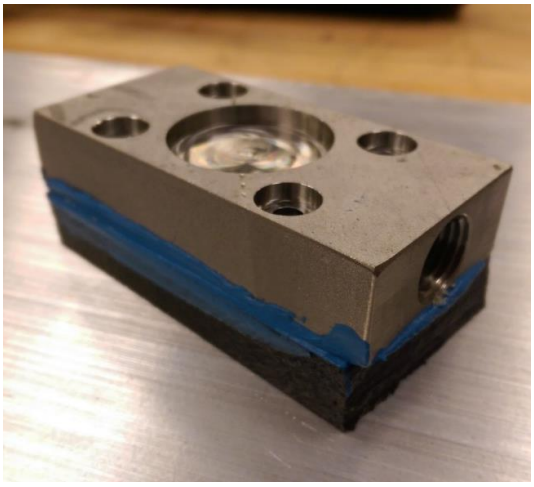

Figure 10: Powder Flow Sensor Mount

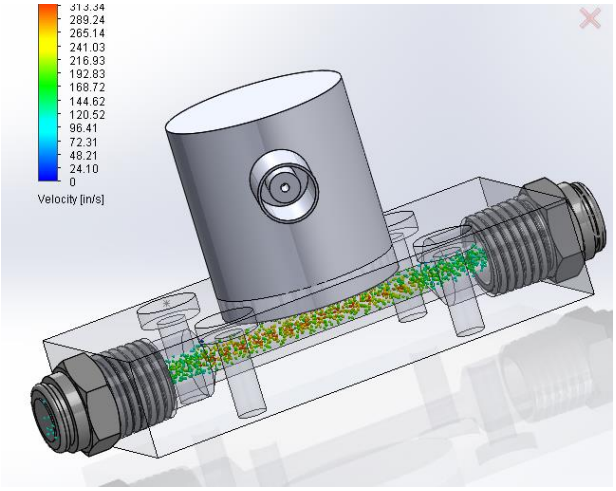

Figure 11: Visualization of Sensor and Mount

4.2 Powder Reservoir Apparatus

The AE signal will be recorded and analyzed, but without an accurate reading of the actual mass flow rate of the powder traveling through the transmission lines, it is impossible to ascertain the accuracy of the AE reading. As previously mentioned, there is no system in place that measures the flow rate of the two-phase fluid used in the LENS process. The powder pneumatically conveyed must be captured while the carrying gas is simultaneously vented. If the gas is not vented, the pressure will build up in the reservoir causing problematic back pressure on the lines and possibly lead to a catastrophic failure. This constraint as well as various others led to the specifications for the design of the powder reservoir apparatus shown below.

- Powder Reservoir Apparatus Design Specifications
    - Separate the two-phase fluid
        - 40 micron brass breather vents: filters allow argon to escape while capturing all of the powder (40-70 micron)
    - Ability to collect each nozzle separately
        - Four separate chambers: each nozzle's two-phase fluid is directed to its respective reservoir
    - Ease of use
        - Flat base: assembly to remain stable while on scale
        - Self-sealing screws: screws with gasket to maintain air-tight seal while still easy to remove to empty
        - Push-to-connect fittings: hoses direct the powder from the nozzles to each reservoir that can be quickly attached/detached
        - Friction fit base: reservoirs fit snugly in their base avoiding any lack of stability and skewed mass flow rates

Figure 12 and Figure 13 contain the CAD models created during the design stage while Figure 14 is a photo of the final build apparatus. The base and the reservoirs were built from ABS plastic to keep cost low and for ease of manufacturing. The remaining components were purchased from an online material supplier.

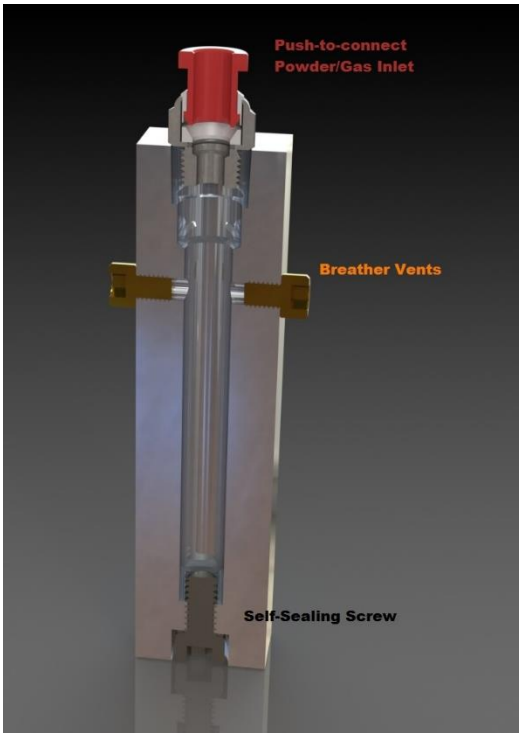

Figure 12: Cross Section of Reservoir

Figure 13: Designed Powder Reservoir

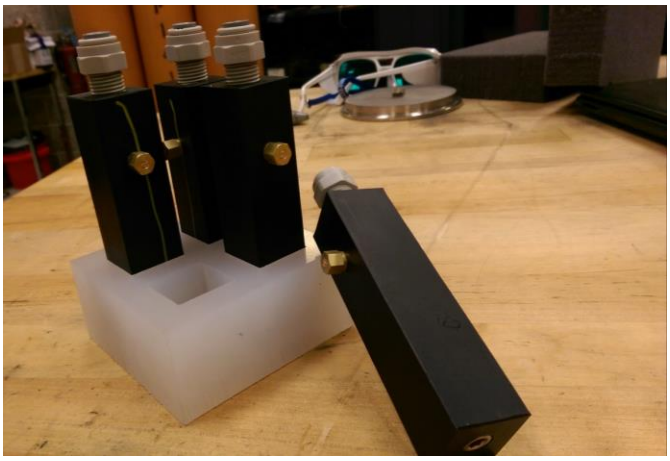

Figure 14: Powder Reservoirs

4.3 Data Acquisition

The powder feeder's setting were changed and held for specific timing intervals in order to test the various flow rates as well as the consistency of the flow rates. These settings and respective times are shown below in Table 3. Acoustic emission from the sensor is recorded at 2MHz while the scale's data is sampled and stored at 10Hz. A Labview VI (visual instrument) was created to query the scale 10 times per second and accurately record the weight and time of each data point. A simple mathematical operation is done to calculate the mass flow rate and is shown in equation **(6)**. The weight (W_{i-1}) of the previous time step is subtracted from the current time step's weight (W_i). This value is then divided by the difference of the time between each data sample.

Table 3: Powder Feeder Settings used in 1st Experiment

Time from beginning of test (s)	0-60	60-120	120-240	240-360	360-540	540-600	600
Powder Feeder Setting	4	6	8	6	4	6	off

$$\boxed{\boldsymbol{Mass\ Flow\ Rate} = \frac{\boldsymbol{W_2 - W_1}}{\boldsymbol{t_2 - t_1}}} \qquad (6)$$

4.4 Data Processing

Initially, the data must be post-processed due to the complex nature of the series of procedures. A Matlab script was written (Appendix A) to load the SQL database containing the AE data and the Labview Measurement File (LVM). The data is loaded and undergoes the conditioning process described in section 2.3 Signal Processing. The scale data is used to calculate the mass flow rate using equation **(6)**. This mass flow rate value is filtered using a moving time average to remove noise. The AE data is sampled using a linear interpolation to match the sample times of the flow rate. Finally, after a time shift, a polynomial is created by a least squares regression. This polynomial is used as a function so that the RMS of the AE data can be used to calculate the mass flow rate in grams/min.

4.5 Set Flow Rate and Powder Feeder Motor Setting

In order to compare the user specified flow rate with the actual mass flow rate, the flow rate of each motor setting must be known. This will allow a comparison of the set and present values of the flow which provides feedback to the LENS operator on the error of the current system condition. These set values are found empirically. The motor's rotational speed is changed in increments of 1 RPM while the mass flow rate is recorded using the scale data acquisition system described previously in section 3.3. Figure 15 illustrates how this is done.

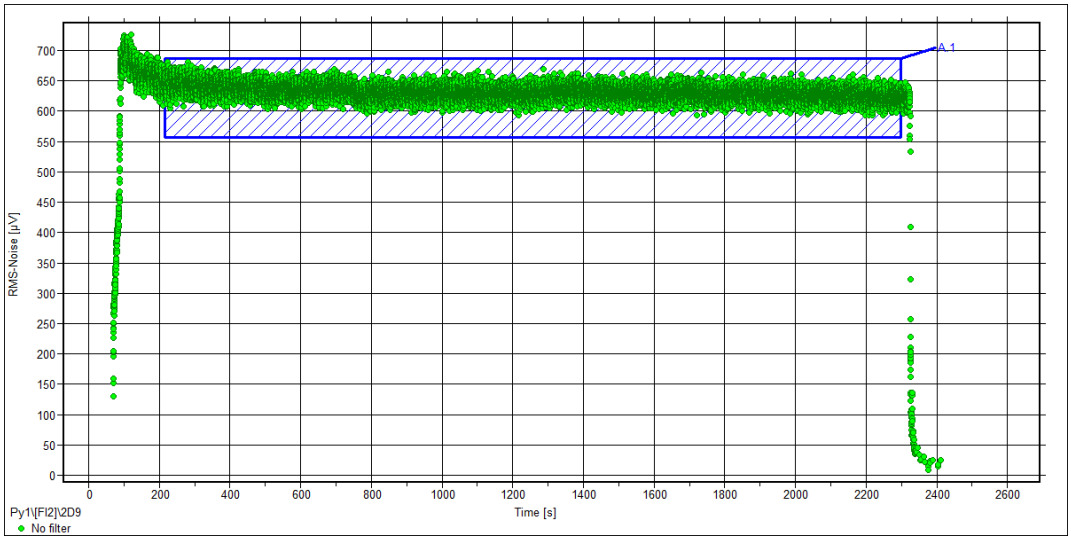

Figure 15: Empirically Extracted Motor-Flow Data

A 'polygon' processor is used in the Vallen software to limit the focus of the analysis to the steady-state portion of the AE data. This will ensure the results are not skewed by the rise and fall times. Note the ramping and eventually settling to a near-steady state condition in Figure 15. The data is averaged over 2000 seconds of data and more than 12 data sets. An average AE RMS is recorded for each motor setting and is used to create an equation describing the flow in terms of the rotational speed of the motor. A linear regression is used to create a first order polynomial. Equation **(7)** describes the set flow rate (SFR) in terms of the motor's rotational speed (RPM).

$$SFR = RPM * 1.748 - 1.0757 \quad (7)$$

4.6 Utilization of Data

The 4th order polynomial provided by the Matlab script (Appendix A) is loaded into the AE test stand. This allows the system to, nearly in real-time, automatically display the current mass flow rate, in grams/min, to the Optomec user. This data is compared to the set powder feeder setting and simultaneously compares the two values. The difference in the set point and the actual can be compared to a user set error limit and an alarm set for when the current difference exceeds the error limit. A BNC (Bayonet Neill–Concelman) cable was used to connect the terminal that takes the control voltage from the Optomec's controller board to one of the Vallen box's inputs. The data is manipulated to provide the set RPM of the powder feeder's motor. This value is used to calculate the set mass flow rate in grams per minute. Figure 16 is a screenshot of the user interface that is displayed while the system is running. The top left plot, in green, contains the power feeder's setting in revolutions per minute. This data must be used to calculate the set flow rate, but is also used to ensure the motor is receiving the appropriate voltage for the set flow. The top right plot, shown in red, is the set flow rate. This is calculated using empirical data on what the flow is at a certain motor rotational speed. The bottom plot, also shown in red, is the actual mass flow rate calculated from the RMS of AE signal. The 3rd order polynomial previously mentioned is used to compute the flow in terms of grams per minute.

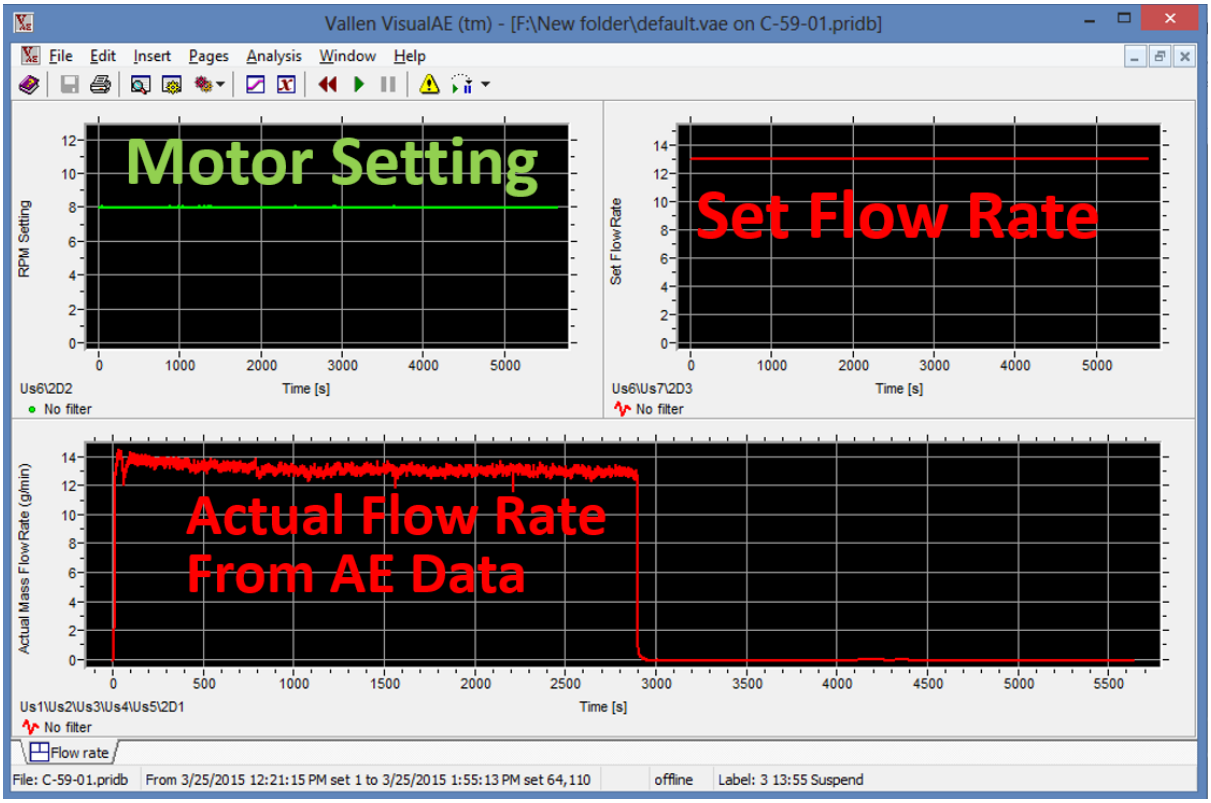

Figure 16: AE User Interface

CHAPTER 4. RESULTS & DISCUSSION

4.1 RMS of AE and Mass Flow Rate

Figure 17 displays the RMS and moving average of the RMS of the AE data. The moving average is shown to simplify the numerous AE hits plotted. The same plot is shown in Figure 18 along with the powder feeder settings denoted. It is obvious the AE data is effected by the change of the powder feeder settings. Figure 19 illustrates the rate of the change in the reservoir's weights. It is also obvious that the AE data and the rate of change of the data from the scale seem to follow the same trends. In order to show this more clearly, the two images were overlaid. The moving average of the AE signal was made opaque so that both plots could be seen. The correlation between the actual mass flow rate and the RMS of the AE data can be seen in these overlaid images shown in Figure 20.

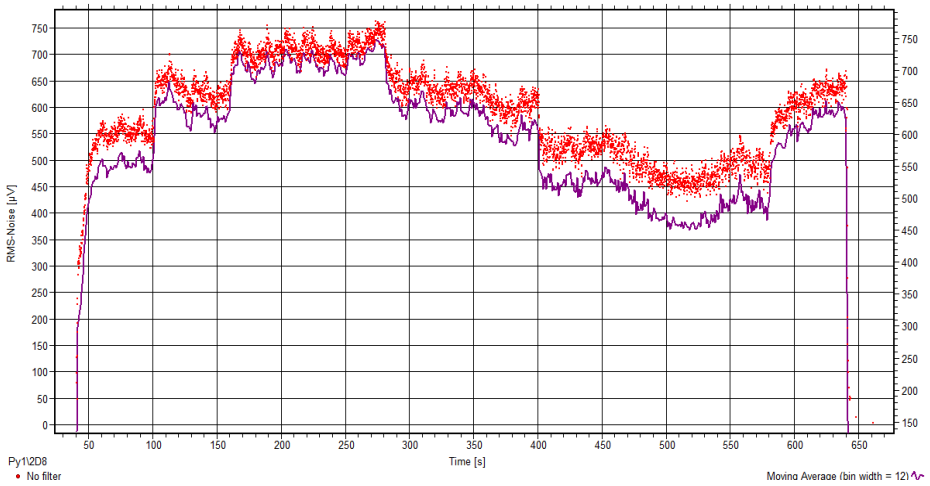

Figure 17: AE signal with Moving Average

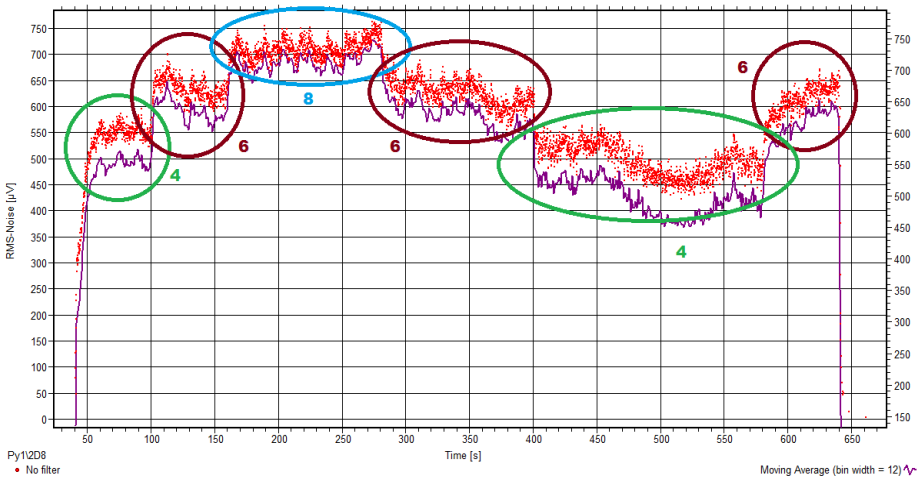

Figure 18: AE signal with Flow rates denoted

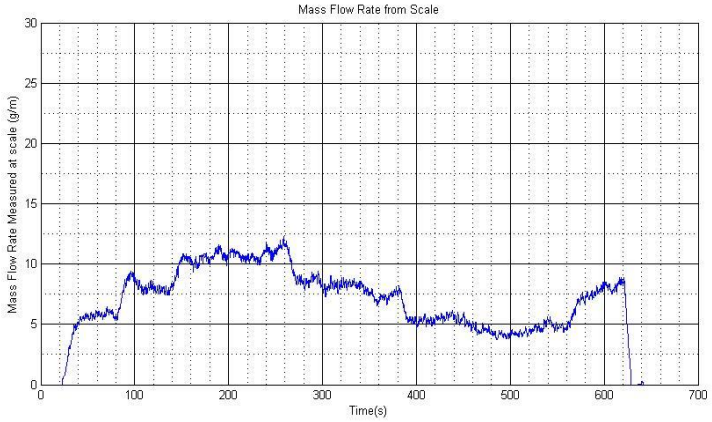

Figure 19: Rate of change of scale weight

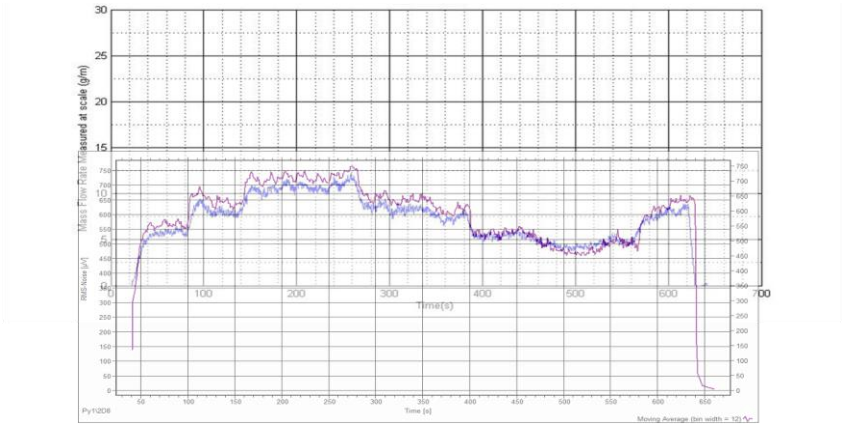

Figure 20: Overlaid Plots of Scale and AE data (1st Experiment)

The unprocessed data is loaded into the Matlab script that conditions the signals so that the relationship may be extracted. While it is obvious the two data sets (i.e. scale and AE) are related (see Figure 20), the form of the equation is not known. Therefore a trial and error approach is taken. The polynomial's order as well as the amount of shifting to be conducted must be optimized. Additionally, there must be a factor that allows each of the trials to be compared to the others. The correlation coefficient, r^2 (see equation **(2)**), is used to quantitatively gauge the accuracy of the trial. Figure 21 represents the outcome of a 3rd order polynomial without using a lag shift. The correlation coefficient is a relatively low .67 since the signals are not aligned. Figure 22 shows the outcome of using a 2nd order polynomial with a lag shift. The correlation coefficient is now .9735, and much closer to being perfectly correlated (i.e. value of 1).

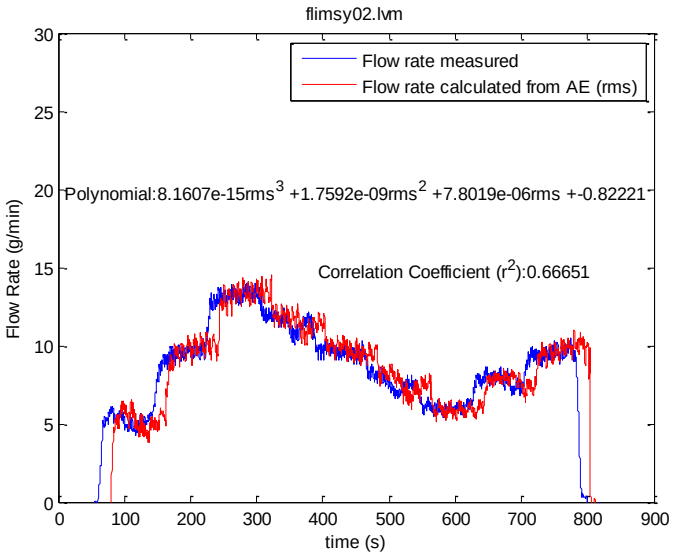

Figure 21: 3rd Order Polynomial Fitting before Lag Shift

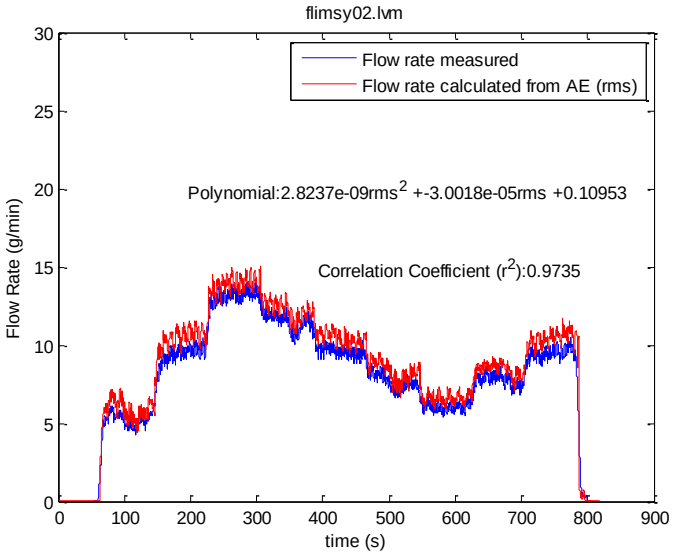

Figure 22: 2nd Order Polynomial with Lag Shift

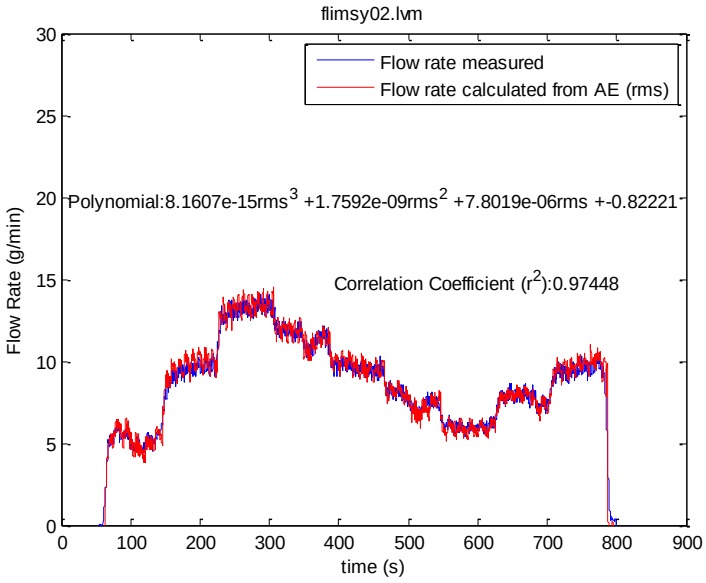

Figure 23: Optimized Formula from Regression

The order of the polynomial was altered while the correlation coefficients were compared. The optimal polynomial was found to be of a 3rd order kind, and the plot using the extracted function is shown in Figure 23. Note the r^2 value of .97448. The contribution of each

polynomial term is presented in the Figure 24's pie chart. The second term, β_2, makes up for nearly 2/3 of the total calculated flow the first term, β_1, also contributes a substantial portion. This prevents one from lowering the order of the polynomial. While this would shorten computation time by simplifying the calculation, it would eliminate the first term propagating error. This is also evident when comparing the correlation coefficients shown in Figure 22 and Figure 23.

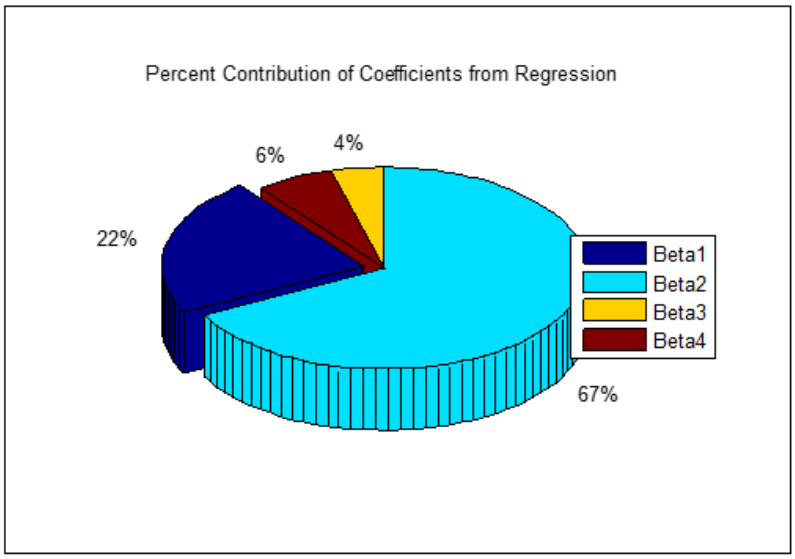

Figure 24: Effect of Coefficients on Flow Calculation

Once the data was collected, it was loaded into the aforementioned Matlab script. Figure 23 illustrates the alignment of the output of the AE RMS and the scale data. The polynomial created is shown in equation **(8)** with the respective coefficients from least squares regression shown in Table 4. This process was done several times to ensure repeatability. Results from two

other experiments are shown in Appendix **Error! Reference source not found.**. They show similar results with different powder setting schedules.

$$\dot{m} = \beta_3 rms^3 + \beta_2 rms^2 + \beta_1 rms + \beta_0 \quad (8)$$

Table 4: Values of Coefficients from Regression

β_3	8.16e-15
β_2	1.76e-9
β_1	7.8e-6
β_0	.822

4.2 Case Study

The mass flow rate sensor has been created and has been shown to be very useful in describing the flow using the AE data from the sensor mount. The system has been used in the LENS process providing feedback on the flow condition for over 200 hours. The following section consists of reports documenting the system's success. Please note some of the figures and data were collected before the implementation of the aforementioned user interface and mathematical relationship. Therefore much of the data is in its raw, unconditioned format.

4.2.1 Noise Isolation

In order to test the system's noise isolation characteristics as well as the robustness of the sensor, data was collected while external vibrations were deliberately introduced. The vibrations

were created by striking the side of the Optomec with a rubber mallet. Figure 25 is a plot of the data from the scale, while Figure 26 contains the AE data recorded using the created system. It is noted that while external vibrations intentionally introduced are pronounced, the noise is not recorded by the AE sensor. The system is likely an excellent candidate for mass flow data in an industrial application in which noise is ubiquitous.

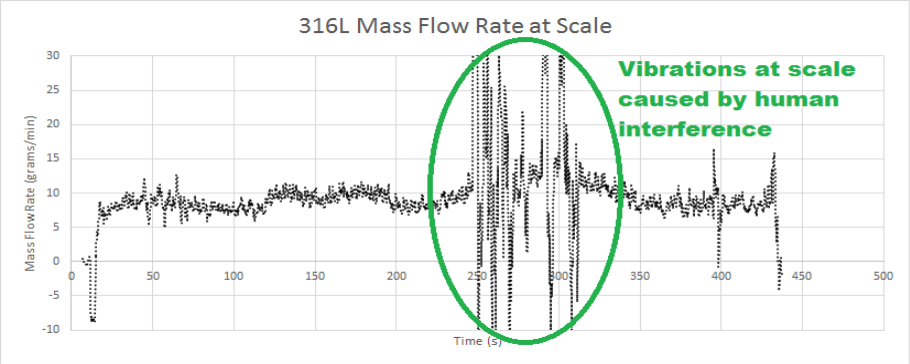

Figure 25: Scale Data with Induced Noise

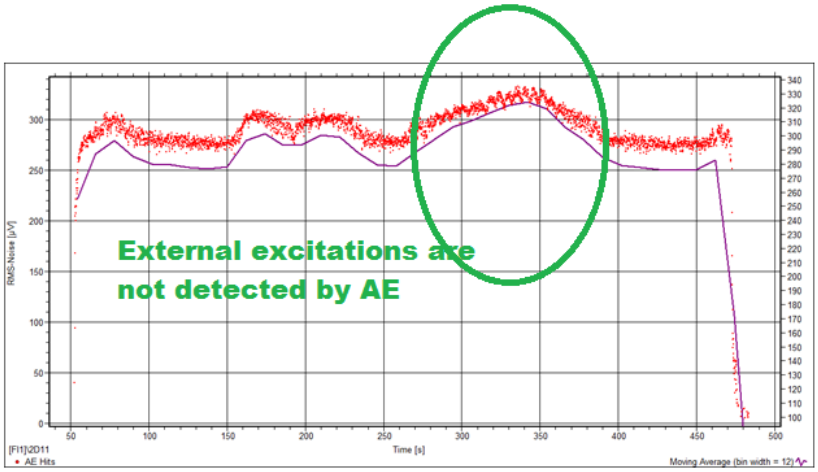

Figure 26: AE Data

4.2.2 Operation Halt

As previously mentioned, the system created has been used during the operation of the LENS process at NIU's ARMM Lab for over 200 hours. It has proven its ability to inform the user of inadequate powder flow. This ability is illustrated in the comparison of Figure 27 and 28 with Figure 29 and 30. The first two of these are the AE data and build outcome, respectively, of a desired LENS operation. The latter two are indicative of a poor flow condition during the build. This knowledge allowed the operator to halt the machine operation saving time and money. The operator found the pressure regulator on the argon tank outlet was set nearly twice as high as normal operation conditions. Note the plot of the RMS in Figure 30 is nearly twice as high as Figure 28.

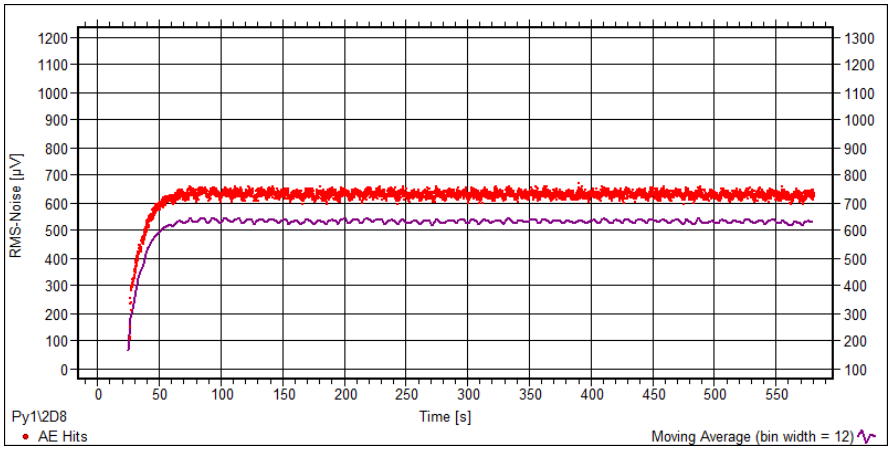

Figure 27: AE Data from Operation with Appropriate Powder Flow

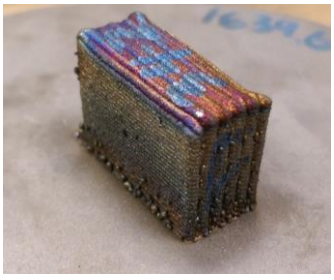

Figure 28: Desired Outcome of Build

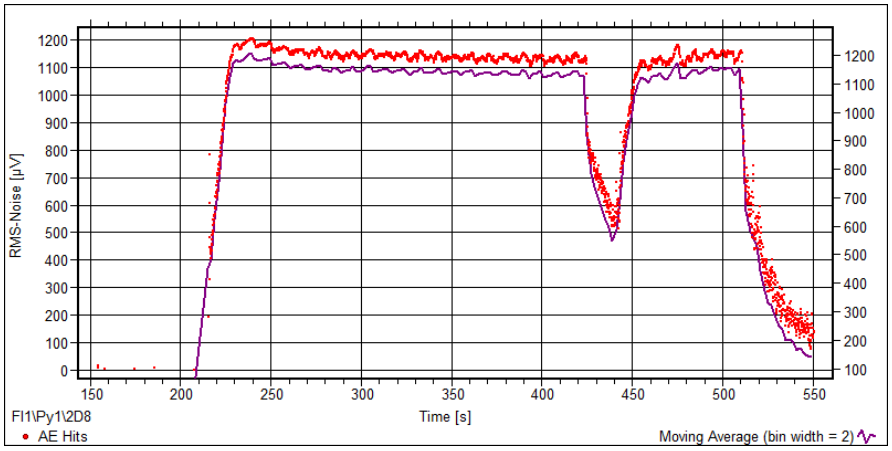

Figure 29: AE Data with Excessive Argon Pressure

Figure 30: Undesired Build Outcome

4.3 Frequency Domain

The AE data is analyzed using a Fast Fourier Transform (FFT) to allow the characterization of the signal in the frequency domain. Since the powder flow is a continuous process and the manner in which the powder is mechanically conveyed is periodic (i.e. rotation of powder feeder's motor), the frequency analysis could provide insight into the condition of the process. This insight may provide a method of improving accuracy.

Matlab code was written that creates a window of frequencies to be analyzed as well as a threshold. A counter keeps track of the amount of times the FFT data crosses the set threshold

within a certain frequency range (i.e. the window). The user interface is shown in Figure 31 with the area of interest inside the dashed red lines. The specified window in the figure has a low end frequency of 500 kHz and a high of 1 MHz. This is used as a quantitative measurement of the frequency domain. While the results proved to trend with the amount of powder being delivered, more work must be done to implement this technique in the LENS process.

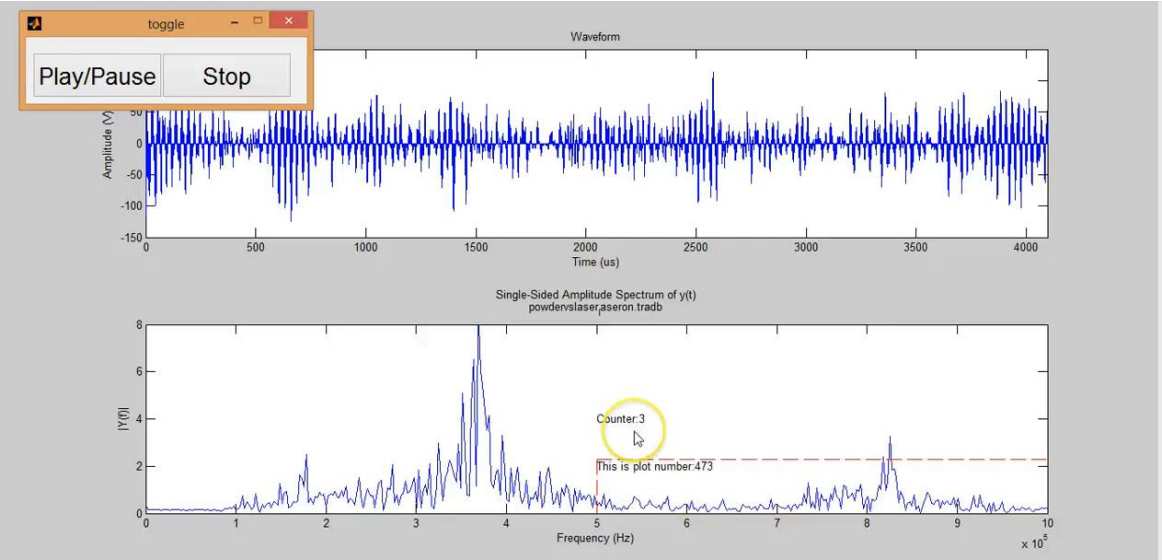

Figure 31: Frequency Domain Windowing and Threshold Crossing Counting

The system developed could prove useful in the post-processing of the AE data. The data can be continuously exported to a computer program that is computing the Fourier Transforms. This data can be used to further characterize the condition of the powder delivery and inform the operator of spatial areas of interest. The current position relative to the AE data that is stored is to be recorded at each time step. During the post-processing, filters can specify outliers in the data and provide the exact location of the areas of interest. Eventually, an integrated system

conducting near real-time FFT's on data sets could provide the operator with in-situ feedback using the frequency domain. This will take substantial effort and time, but could provide a more robust look into the powder delivery process.

CHAPTER 5. CONCLUSIONS AND FUTURE WORK

The work accomplished lays the groundwork for individual nozzle monitoring and control. This report has shown the robust ability of acoustic emission to be used as a multi-phase fluid flow meter. It has been proven to work in the presence of external noise as well as with variations in the density of the multi-phase fluid flow present in the LENS's powder delivery. While this report focused on its application in the LENS process the technology could be applied to countless other industrial applications. The Matlab software, along with the powder reservoir apparatus, allow an operator to calibrate their system to ensure accurate and repeatable feedback on a system's real-time mass flow rate. While this system has shown repeatability, the reproduction of the mount might cause changes in the system's physical properties and therefore alter the attenuation of the AE pressure waves. The Matlab code automatically analyzes the data, compares it to the actual mass flow rate (from the scale data), and creates the characteristic n^{th} order polynomial. This allows the user to calibrate this mass flow meter to their specific machine which provides corrections for any environmental changes such as variations in the ambient temperature, pressure or humidity.

5.1 Individual Nozzle Monitoring

The main issue with attempting to monitor each nozzle is LENS's build chamber environment. The chamber, especially near the deposition location, gets very hot. Temperatures reach 1400ºC. The AE sensors cannot be exposed to this type of temperature nor the thermal shock present near the build location. A method of monitoring the flow externally must be used.

As previously mentioned, there are multiple modes AE waves travel. One grouping of these modes is dubbed 'Plate Waves'. Rather than portions of the medium transmitting the wave to another location, the entire medium acts as a guide for the wave. This phenomena allows one to use a 'waveguide' to remotely collect AE signals.

A waveguide has been designed to be installed in to the deposition head. The design, shown in Figure 32, will guide the pressure waves created by the powder delivery towards the sensor shown in Figure 33. The load disc will allow a male threaded insert to apply force to the guide's base. This force can be adjusted and will ensure proper coupling at the base's underside.

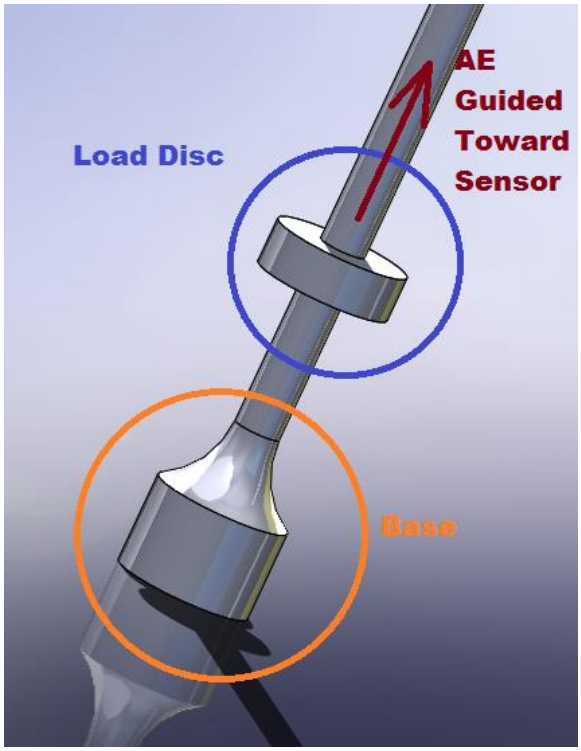

Figure 32: Waveguide Base

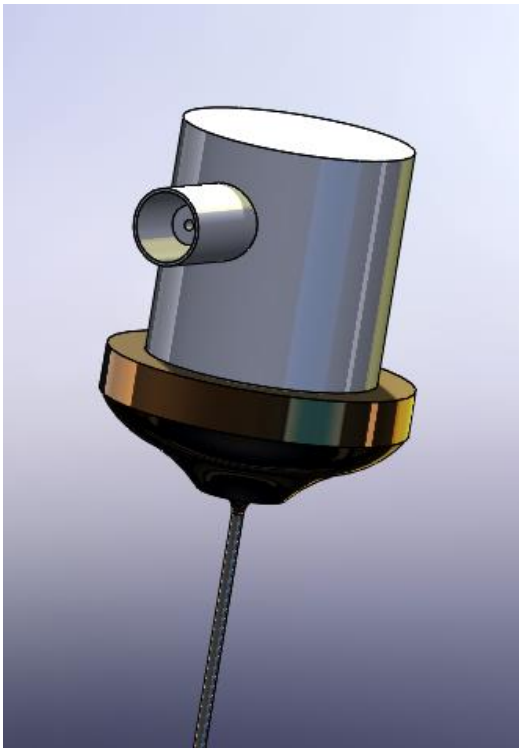

Figure 33: AE Sensor on Waveguide

5.2 Design of New Deposition Head

The deposition head must be modified to accept the waveguides. The original head and lower portion are shown in Figure 34, Figure 35, and Figure 36, whereas the proposed modifications are displayed in Figure 37 and Figure 38. Note the manner in which the powder is routed. The final divide, that creates the four powder delivery channels, is located near the lower portion of the head. The waveguides must be placed near this junction.

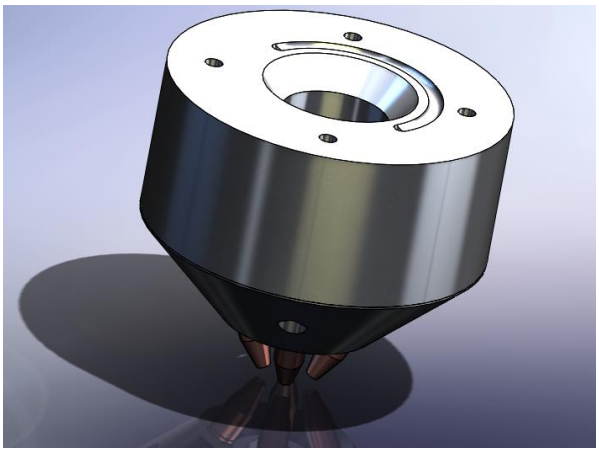

Figure 34: Original Deposition Head

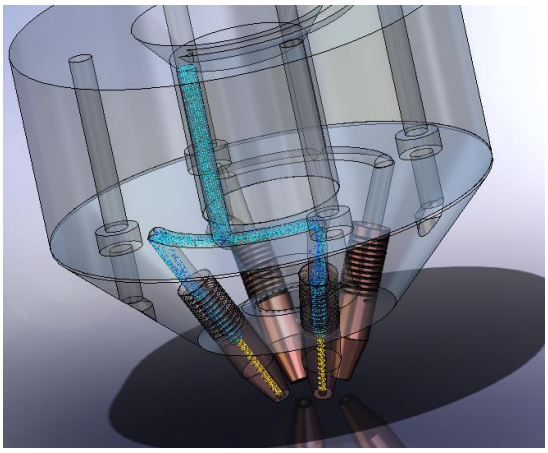

Figure 35: Internal Flow Channels

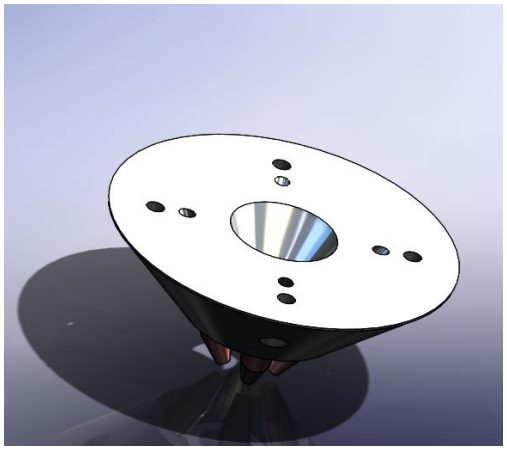

Figure 36: Original Deposition Head Lower Section

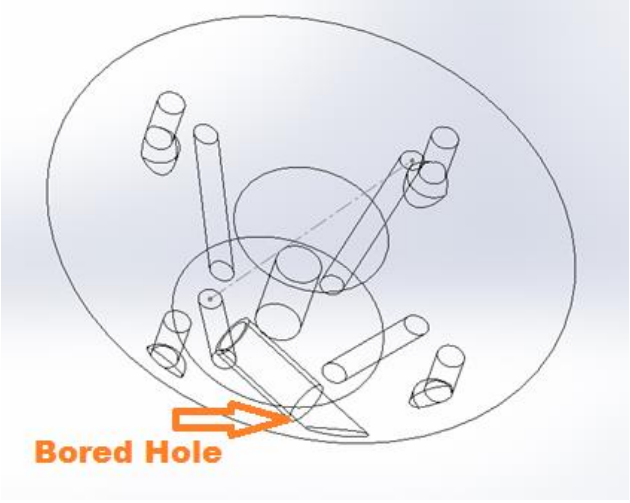

Figure 37: Lower Deposition Head Modification

The bored hole shown in Figure 37 will be tapped and threaded to allow the abovementioned threaded insert to be attached. The insert will apply a force on the load disc which will push the base of the guide against the floor of the bored hole. The AE is guided along the wire that is attached to the sensor's mounting base. This mounting platform can be remotely located to avoid the harsh conditions near the build location.

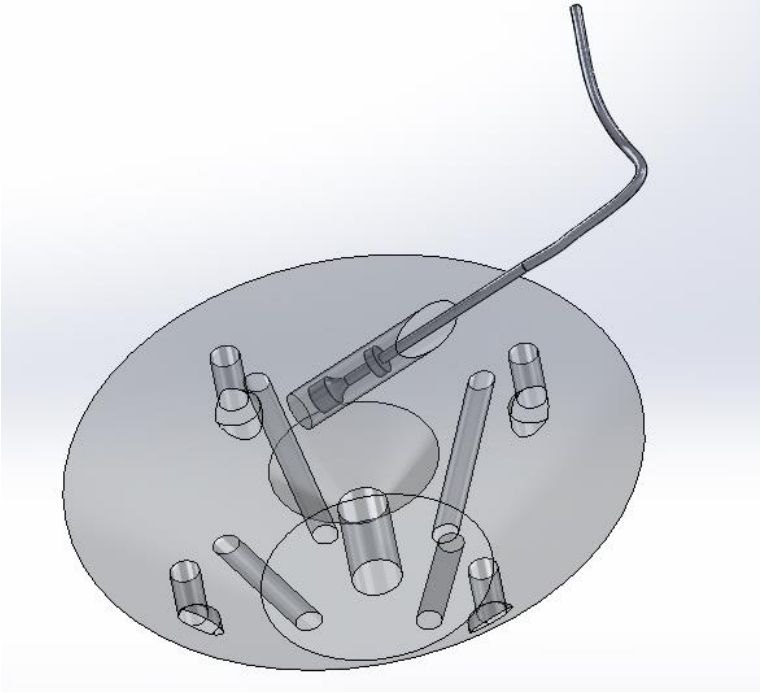

Figure 38: Lower Deposition Head with Waveguide

REFERENCES

[1] Copeland, Micheal V. "DIY Market Slows Dramatically as 3-D Printing Hits Its Industrial Stride" Wired Magazine. http://www.wired.com/2013/05/3d-printing-hits-its-industrial-stride-while-the-diy-market-slows-dramatically/.

[2] W. Hofmeister, M. Wert. Investigating Solidification with the Laser-Engineered Net Shaping (LENS™) Process. *JOM*. July 1999 (vol. 51, no. 7).

[3] Miller R. K. Nondestructive Testing Handbook: Volume 5 *Acoustic Emission Testing*. American Society for Nondestructive Testing, Ohio, 1987.

[4] Miinshiou Huang, Liang Jiang, Peter K. Liaw, Charlie R. Brooks, Rodger Seeley, and Dwaine L. Klarstrom. Using Acoustic Emission in Fatigue and Fracture Materials Research. JOM. November 1998 (vol. 50, no. 11).

[5] *Introduction to Acoustic Emission Testing.* Non-destructive Resource Center. https://www.nde-ed.org

[6] Addali, A., Al-lababidi, S., Yeung, H., Mba, D., & Khan, F. (2010). Acoustic emission and gas-phase measurements. *Proceedings of The Insitution of Mechanical Engineers*.

[7] J. Whiting, F. Sciammarella. Monitoring Tool Wear During Micro End Milling Using Acoustic Emission. *ICCEES 2014 Conference Proceedings.* June 2014.

[8]Y. Yan. Mass Flow Measurement of Bulk Solids in Pneumatic Pipelines. *Measurement Science and Technology.* (vol. 7, 1996) pp. 1687-1706.

[9] E. Ehrhardt, M. Montagne, H. Berthiaux, B. Dalloz-Dubrujeaud, C. Gatumel. Assessing the Homogeneity of Powder Mixtures by On-Line Electrical Capacitance. *Chemical Engineering and Processing* (vol. 44, 2005) pp. 303-313.

[10] P. Wypych. Dilute-Phase Pneumatic Conveying Problems and Solutions. *Handbook of Conveying and Handling of Particulate Solids.* Elsevier Science. 2001.

[11] T. Abberger, M. Adams, D. Medrano, et al. Granulation. *Handbook of Powder Technology*. Volume 11, 2007.

[12] N. Pohlman, B. Serverson, et al. Surface Roughness Effects in Granular Matter: Influence of Angle of repose and the Absence of Segregation. *Physical Review.* E 73. 2006

[13]W.H.Pres et al, Numerical Recipes, Cambridge University press, 1992

[14] M. B. Rhudy. Real Time Implantation of a Military Impulse Noise Classifier. University of Pittsburgh, 2009.

[15] NIST/SEMATECH e-Handbook of Statistical Methods, http://www.itl.nist.gov/div898/handbook/, 2/11/2015.

APPENDIX A

MATLAB SCRIPT

```
      %%%% Script to shift the time of data from scale to match AE data %%%%
      %%%%%%%%%%%%%%%%%%%%%%%%%% Justin Whiting%%%%%%%%%%%%%%%%%%%%%%%%%%%%%%
      % close all
      clearvars -except p
      [fileAE , rmss,time] = loadvallendata('pr') %% Load in Acoustic
Emission Data by calling function loadvallendata; RMS and time of each AE hit
      time = time*10^-7; %% Convert time into seconds

      [filename,pathname] = uigetfile('*.*','MultiSelect', 'on'); %% Prompt
user to select which file for weight of reservoir
      fid = fopen(strcat(pathname,filename));
      L = cell2mat(textscan(fid,'%f %f', 'headerlines', 22));


      for i=1:length(L)-1 %% Compute mass flow rate by using time steps and
weight data
          L(i,3) = 60*(L(i+1,2)-L(i,2)) / (L(i+1,1) - L(i,1));
      end
      scale = smooth(L(:,3),77); %% Filter data to eliminate spiking
      ldiff = abs(length(rmss)-length(scale));
      timesc = L(:,1);
       if length(rmss) > length(scale)
           %L(length(scale):length(rmss))=0;
             scale(length(scale):length(rmss))=0;
           timesc(length(scale):length(rmss))=0;
           scale = circshift(scale,ldiff+1);
      timesc = circshift(timesc,ldiff+1);
      timesc(1:ldiff+1) = linspace(0,timesc(ldiff+2)-.0001,ldiff +1);
       else
           rmss(length(rmss):length(scale))=0;
           time(length(time):length(scale))=0;
           rmss = circshift(rmss,ldiff+1);
      time = circshift(time,ldiff+1);
      time(1:ldiff+1) = linspace(0,time(ldiff+2)-.0001,ldiff +1);
       end



      rms = interp1(time, rmss , timesc);
      [acor,lag] = xcorr(scale,rms);
      [C,I] = max(acor)
      diffe = lag(I);
      timesc = L(:,1);
      if diffe < 0
          for i =1:length(scale)+diffe -1
            %  if  isempty(rmss(i+abs(diffe)))
                %  break
              %else
              scale(i) = scale(i+abs(diffe));
              %end
          end
```

```
end

p= polyfit(rms,scale,3)
timerms = timesc -35.5;
rmscheck = polyval(p,rms);
% figure
rmscheck = smooth(rmscheck)
plot(timesc,scale)
hold on
plot(timerms, rmscheck,'r')
axis([0 1000 0 30])
axis 'auto x'
title(filename)
xlabel('time (s)')
ylabel('Flow Rate (g/min)')
legend('Flow rate measured', 'Flow rate calculated from AE (rms)')
```

APPENDIX B

ACOUSTIC EMISSION SENSOR MOUNT

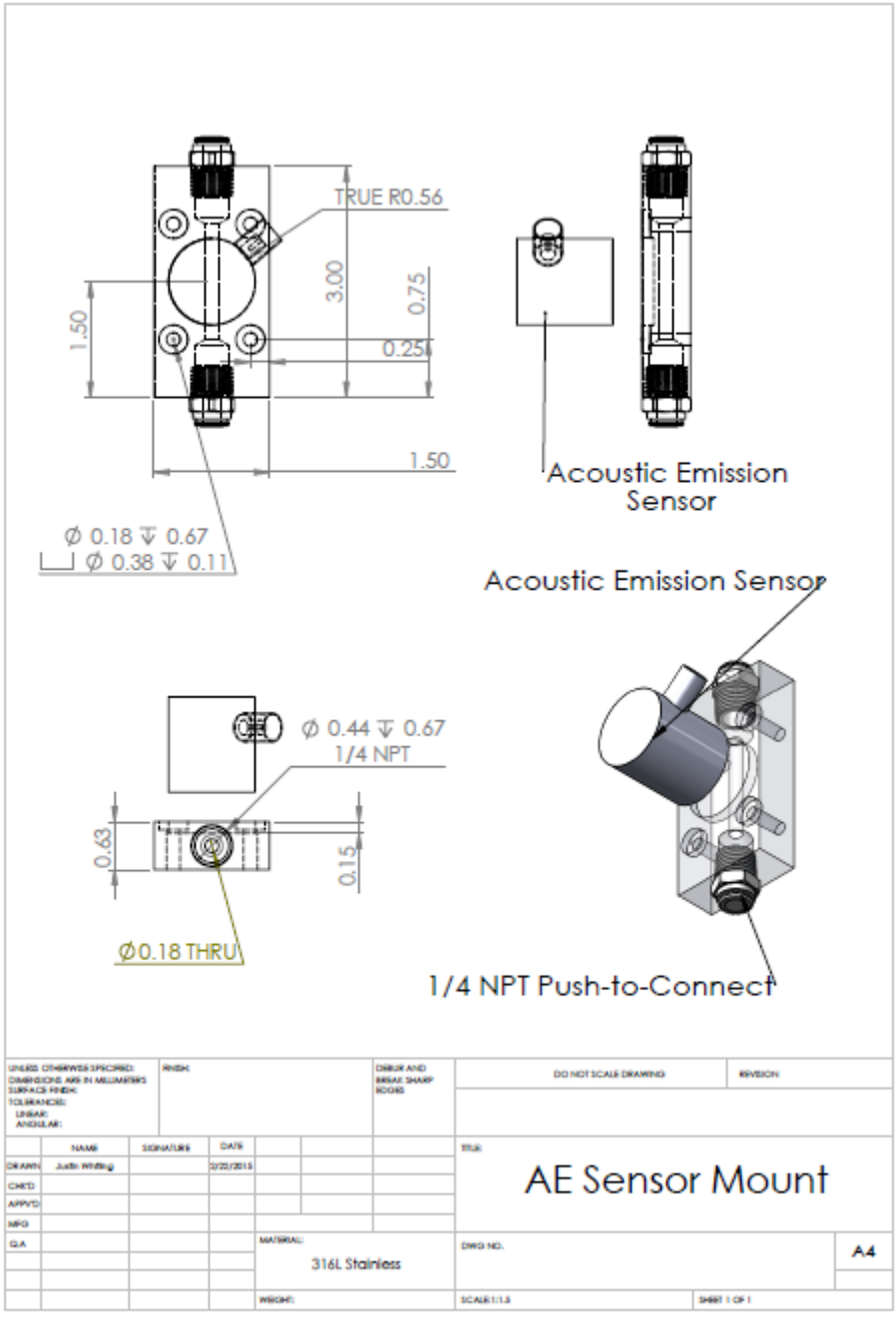
TRUE R0.56
3.00
0.75
0.25
1.50
1.50
Ø 0.18 ↧ 0.67
⌴ Ø 0.38 ↧ 0.11
Acoustic Emission Sensor
Acoustic Emission Sensor
Ø 0.44 ↧ 0.67
1/4 NPT
0.63
0.15
Ø0.18 THRU
1/4 NPT Push-to-Connect
UNLESS OTHERWISE SPECIFIED:
DIMENSIONS ARE IN MILLIMETERS
SURFACE FINISH:
TOLERANCES:
LINEAR:
ANGULAR:
FINISH:
DEBUR AND BREAK SHARP EDGES
DO NOT SCALE DRAWING
REVISION
NAME
SIGNATURE
DATE
DRAWN
Justin Whitley
2/22/2016
CHK'D
APPV'D
MFG
Q.A
TITLE:
AE Sensor Mount
MATERIAL:
316L Stainless
DWG NO.
A4
WEIGHT:
SCALE:1:1.5
SHEET 1 OF 1

APPENDIX C

RESULTS FROM EXPERIMENTS 2 & 3

Table 5: Powder Feeder Settings used in 2nd Experiment

Time from beginning of test (s)	0-80	80-160	160-240	240-320	320-400	400-480	480-560	560-640	640-720	720
Powder Feeder Setting	4	6	8	7	6	5	4	5	6	off

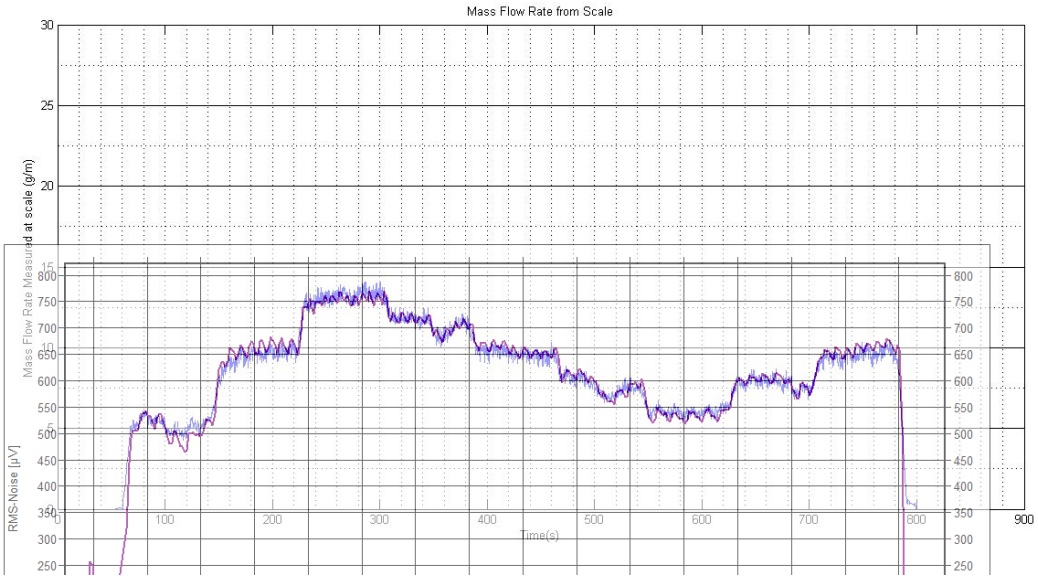

Figure 39: Overlaid Plots of Scale and AE data (2nd Experiment)

Table 6: Powder Feeder Settings used in 3nd Experiment

Time from beginning of test (s)	0-90	90-180	180-270	270-360	360-450	450-540	540
Powder Feeder Setting	4	6	8	6	4	8	off

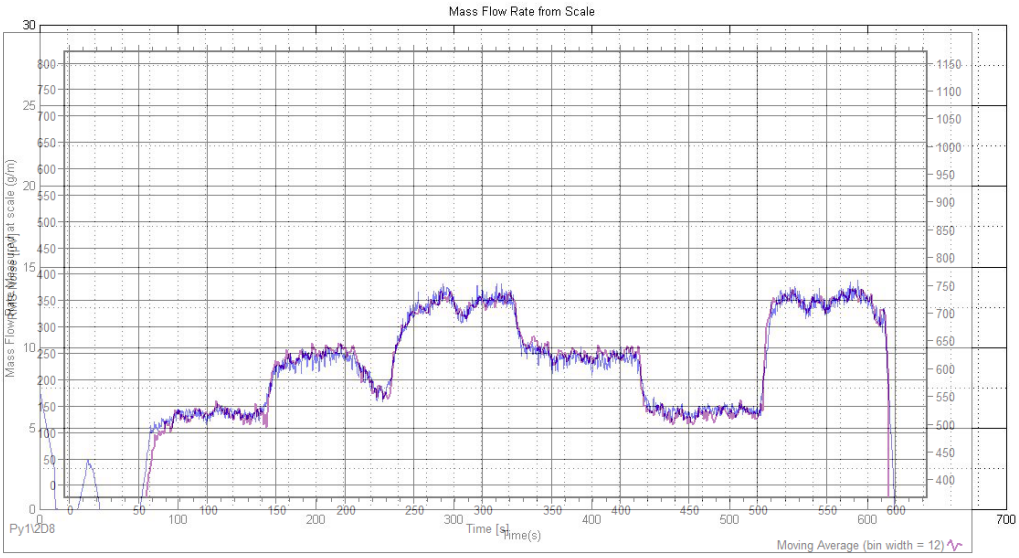

Figure 40: Overlaid Plots of Scale and AE data (3nd Experiment)